

Triaxial shapes in the interacting vector boson model

H. G. Ganev

Institute of Nuclear Research and Nuclear Energy, Bulgarian Academy of Sciences, Sofia BG-1784, Bulgaria and Bogoliubov Laboratory of Theoretical Physics, Joint Institute for Nuclear Research, Dubna RU-141980, Moscow Region, Russia

(Received 14 July 2011; revised manuscript received 17 October 2011; published 21 November 2011)

A new dynamical symmetry limit of the two-fluid interacting vector boson model (IVBM), defined through the chain $\text{Sp}(12, R) \supset \text{U}(3, 3) \supset \text{U}^*(3) \otimes \text{SU}(1, 1) \supset \text{SU}^*(3) \supset \text{SO}(3)$, is introduced. The $\text{SU}^*(3)$ algebra considered in the present paper closely resembles many properties of the $\text{SU}^*(3)$ limit of the interacting boson model-2, which have been shown by many authors geometrically to correspond to the rigid triaxial model. The influence of different types of perturbations on the $\text{SU}^*(3)$ energy surface, in particular the addition of a Majorana interaction and an $\text{O}(6)$ term to the model Hamiltonian, is studied. The effect of these perturbations results in the formation of a stable triaxial minimum in the energy surface of the IVBM Hamiltonian under consideration. Using a schematic Hamiltonian that possesses a perturbed $\text{SU}^*(3)$ dynamical symmetry, the theory is applied for the calculation of the low-lying energy spectrum of the nucleus ^{192}Os . The theoretical results obtained agree reasonably with the experimental data and show a very shallow triaxial minimum in the energy surface for the ground state in ^{192}Os , suggesting that the proposed dynamical symmetry might be appropriate for the description of the collective properties of different nuclei, exhibiting triaxial features.

DOI: [10.1103/PhysRevC.84.054318](https://doi.org/10.1103/PhysRevC.84.054318)

PACS number(s): 21.60.Ev, 21.60.Fw, 27.80.+w

I. INTRODUCTION

It has been known for a long time that in certain mass regions nuclei with static deformation show deviations from a rigid axially symmetric picture. The possibility of static triaxial shapes for the ground state of nuclei is a long-standing problem in nuclear structure physics despite the fact that very few candidates have been found experimentally [1,2]. In the geometrical approach the triaxial nuclear properties are usually interpreted in terms of either the γ -unstable (or γ -soft) rotor model of Wilets and Jean [3] or the rigid triaxial rotor model of Davydov *et al.* [4]. These models exploit the geometrical picture of the nucleus according to the collective model (CM) of Bohr and Mottelson, expressed in terms of the intrinsic variables β and γ where the former specifies the ellipsoidal quadrupole deformation and the latter the degree of axial asymmetry. To describe the deviations from axial symmetry the model of Wilets and Jean assumes that the potential energy is independent of the γ degree of freedom, whereas in the model of Davydov *et al.* one considers a harmonic oscillator potential with a minimum at finite values of γ producing a rigid triaxial shape of the nucleus.

Recently, analytical solutions of the Bohr Hamiltonian regarding the triaxial shapes using the Davidson potential [5] and the sextic oscillator [6] were obtained, where the triaxial shapes are assumed from the very beginning. The former, called the Z(5)-D solution, is shown to cover the region between a triaxial vibrator and the rigid triaxial rotator, whereas the Z(5) solution corresponds to the critical point of the shape phase transition from a triaxial vibrator to the rigid triaxial rotator. Triaxiality was also studied in the framework of the algebraic collective model [7], and the onset of rigid triaxial deformation was considered [8].

An alternative description of nuclear collective excitations is provided by the interacting boson model (IBM), which, in contrast to the geometrical models, is of an algebraic

nature. To accommodate the triaxial shapes in the IBM, several approaches can be adopted. It was shown that the triaxial shapes can occur in three different cases:

- (1) In the IBM-1 framework, in which no distinction between protons and neutrons is made, the inclusion of higher-order (three-body) terms is needed [9,10].
- (2) In the *sdg*-IBM framework (using *s*, *d*, and *g* bosons), the presence of the *g* boson also suffices [11,12].
- (3) In the IBM-2 framework, in which protons and neutrons are used as distinct entities, the inclusion of one- and two-body terms suffices [13–16].

In the IBM-1 framework the triaxial shapes are usually obtained by adding three-body terms of the type $[d^\dagger d^\dagger d^\dagger]^{(L)} \cdot [\tilde{d}\tilde{d}\tilde{d}]^{(L)}$ (see, e.g., Ref. [9]). These terms generate a relatively broad region of triaxiality in the parameter space of the Hamiltonian. In Ref. [17] it is shown that by adding to the consistent- Q formalism Hamiltonian a cubic combination $(\hat{Q} \times \hat{Q} \times \hat{Q})^{(0)}$ of the most general quadrupole operator \hat{Q}^χ coupled to zero angular momentum, called the cubic consistent- Q Hamiltonian, there exists a very tiny region of triaxiality around $\chi \approx \pm\sqrt{7}/2$ between the prolate and oblate phases. The \hat{Q} cubic term is interpreted as a correction to the quadrupole-quadrupole scalar product, which in combination with the latter can generate stable triaxial shapes.

The study of the effects of various multipole interactions within the framework of the *sdg*-IBM on the equilibrium shape of the ground state in deformed nuclei has revealed that a hexadecapole interaction involving a *g* boson is needed to induce a triaxial shape. Over the years, microscopic and phenomenological evidence has been gathered that shows the importance of the *g* boson in deformed regions. Including the *g* boson, in a recent study in the *sdg*-IBM, no shape or phase transitions toward stable triaxial shapes were found [12].

An important feature offered by the IBM-2 [18] is the possibility to get triaxial shapes [13–16] in addition to the

axially symmetric ones, only taking into account explicitly the proton-neutron degrees of freedom or the two-fluid character of the nuclear system. The triaxial shapes then arise as a result of different deformations of the proton and neutron fluids. The microscopic conditions leading to two-fluid triaxial structure are found when the proton bosons are particle-like (i.e., below mid-shell) and the neutron bosons are hole-like (above mid-shell) or vice versa. A new critical-point $Y(5)$ symmetry [19] from axially deformed to triaxial shapes was proposed and suggested to be of importance in considering triaxial shapes in the phase diagram of the IBM-2.

In the present paper we exploit an algebraic approach, complementary to IBM, for the description of triaxial nuclei and show how within the framework of the phenomenological interacting vector boson model (IVBM) one might obtain triaxial shapes. The IVBM and its recent applications for the description of diverse collective phenomena in the low-lying energy spectra (see, e.g., the review article [20]) exploit the symplectic algebraic structures and the $Sp(12, R)$ is used as a dynamical symmetry group. Symplectic algebras have been applied extensively in the theory of nuclear structure. They are used generally to describe systems with a changing number of particles or excitation quanta and in this way provide for larger representation spaces and richer subalgebraic structures that can accommodate the more complex structural effects as realized in nuclei with nucleon numbers that lie far from the magic numbers of closed shells.

The symplectic symmetries emerge as appropriate dynamical symmetries for the many-body theory of collective motion, considering the nucleus from a hydrodynamic perspective [21]. For example, the one-fluid symplectic model of Rowe and Rosensteel [22], based on the non-compact dynamical algebra $Sp(6, R)$, allows for the description of rotational dynamics in a continuous range from irrotational to rigid rotor flows. The extension of the $Sp(6, R)$ symplectic model to the case of two-fluid nuclear systems leads naturally to the $Sp(12, R)$ dynamical symmetry. In this respect the symplectic IVBM can be considered as a generalization of the symplectic model of Rowe and Rosensteel (contained as a submodel of the $Sp(12, R)$ IVBM) when the nuclear many-body system is viewed as consisting of two different interacting subsystems.

The different shapes that take place within the framework of the two-fluid IVBM were investigated in Ref. [23]. It was shown that there exist three distinct shapes corresponding to the three dynamical symmetries of IVBM: (1) spherical shape, $U_p(3) \otimes U_n(3)$; (2) γ -unstable deformed shape, $O(6)$; and (3) axially deformed shape, $SU(3) \otimes U_T(2)$. It turns out that these are not all the possible shapes associated with the algebraic structures of the IVBM that might arise. The aim of this paper is to show that the IVBM possesses a very rich phase structure, which also contains, beyond the spherical and axially deformed shapes, triaxial shapes. For this purpose we propose a different dynamical symmetry limit of the IVBM, which in some aspects is related to one of the dynamical symmetries of the IBM-2, namely the $SU^*(3)$ one. The $SU^*(3)$ limit of IBM-2 was discussed extensively in Refs. [24–26]. The latter gives rise to the Dieperink tetrahedron [13], which has an extra dimension compared to the Casten triangle [27], and to a new, triaxial shape phase of the model.

It was shown in the literature that the exact $SU^*(3)$ symmetry possesses a large degeneracy in the level spectra which in actual nuclei is not observed and hence the $SU^*(3)$ symmetry probably does not appear in its pure form and must be perturbed. In many cases, the energy spectra exhibit transitional patterns and might be situated between the $SU^*(3)$ and $O(6)$ or $SU(3)$ and $SU^*(3)$ dynamical limits. In this respect, we study the influence of different types of perturbations on the $SU^*(3)$ dynamical symmetry energy surface of the IVBM. It is shown that the proposed dynamical symmetry limit might be of relevance for the description of the collective properties of different nuclei exhibiting triaxial features.

II. THE ALGEBRAIC STRUCTURE OF THE NEW DYNAMICAL SYMMETRY

It was suggested by Bargmann and Moshinsky [28] that two types of bosons are needed for the description of nuclear dynamics. They showed that the consideration of only a two-body system consisting of two different interacting vector particles will suffice to give a complete description of N three-dimensional oscillators with a quadrupole-quadrupole interaction. The latter can be considered as the underlying basis in the algebraic construction of the *phenomenological* IVBM.

The algebraic structure of the IVBM [20,23,29] is realized in terms of creation and annihilation operators of two kinds of vector bosons $u_m^\dagger(\alpha)$, $u_m(\alpha)$ ($m = 0, \pm 1$), which differ in an additional quantum number $\alpha = \pm 1/2$ (or $\alpha = p$ and n)—the projection of the T -spin (an analog to the F -spin of IBM-2 or the I -spin of the particle-hole IBM). In the present paper, we consider these two bosons just as elementary building blocks or quanta of elementary excitations (phonons) rather than real fermion pairs, which generate a given type of algebraic structures. Thus, only their tensorial structure is of importance and they are used as an auxiliary tool, generating an appropriate *dynamical* symmetry. These elementary excitations carry an angular momentum $l = 1$; that is, they transform as vectors with respect to the rotational group $SO(3)$. In this regard, the s and d bosons of the IBM-1 can be considered as bound states of elementary excitations generated by the two vector bosons.

The microscopic foundation of the IVBM is beyond the scope of the present paper. (A short discussion on this matter can be found in Ref. [20].) Nevertheless, some remarks concerning this topic can be very useful for the readers who are not familiar with the IVBM.

It is known that the IBM is now standard and the s and d bosons are viewed as working approximations of the composite S and D bosons made up of nucleons held together by the pairing and quadrupole forces. Additional degrees of freedom are further incorporated in the extended versions of the model (e.g., the inclusion of p , f , and g bosons; the inclusion of the isospin, the F -spin and the particle-hole I -spin). In this respect, the natural question about the connection between the IVBM and the standard versions of IBM arises. The answer is obtained [30] by means of the boson mapping technique, which is widely applied to the problems of microscopic foundation of the IBM [31]. It is shown [30]

that the IVBM boson space can be mapped on the ideal boson space of the IBM, including, beyond the standard s and d bosons (IBM-1), also the p bosons. The latter (together with the f bosons) are shown to play a crucial role in the description of the deformed asymmetric shapes in nuclei, in which the octupole and dipole (cluster) degrees of freedom must be taken into account. This specific version of the IBM is denoted as IBM-3.5 (intermediate between IBM-3 and IBM-4). The interaction between these secondary s , d , and p bosons is induced by the interaction between the vector bosons.

A similar situation occurs also in the specific isospin-invariant version of the fermion dynamical symmetry model [32] applied to the sd -shell nuclei, in which the states constructed from the nucleon pairs are built from two p -objects ($l = 1$), as well as in the IVBM.

The introduction of a p boson (p -object) in nuclei with mixed quadrupole-octupole deformation has been pointed out by many authors, including also microscopic considerations [33,34]. The need for the p boson was suggested by schematic shell-model calculations [35], in which collective pairs of both positive (S and D pairs) and negative parity (P and F pairs) are used as building blocks. The p boson has been introduced in different studies of clustering phenomena in nuclei as well, where the dipole degrees of freedom are connected with the relative motion of the clusters [36].

In the most general case the two-body model Hamiltonian should be expressed in terms of the generators of the group $\text{Sp}(12, R)$. In addition to the non-compact ‘‘symplectic dynamical symmetry limits’’ (subgroup chains starting with some of the symplectic subalgebras of $\text{Sp}(12, R)$; see Refs. [20,37]), in some special cases the two-body model Hamiltonian can be written in terms of the generators of the subgroups of the maximal compact subgroup $\text{U}(6) \subset \text{Sp}(12, R)$ only. The following lattice of group-subgroup chains of $\text{Sp}(12, R)$ takes place (excluding the ‘‘symplectic limits’’ given in Refs. [20,37]):

$$\begin{array}{ccccccc}
 & & & & \text{U}(3) \otimes \text{U}_T(2) & \longrightarrow & \text{SU}(3) \otimes \text{U}_T(2) \\
 & & & & \searrow & & \searrow \\
 & & & & \text{O}_\pm(6) & \longrightarrow & \overline{\text{SU}}_\pm(3) \otimes \text{SO}(2) \\
 & & & & \searrow & & \searrow \\
 \text{Sp}(12, R) & \nearrow & \text{U}(6) & \longrightarrow & \text{U}_p(3) \otimes \text{U}_n(3) & \longrightarrow & \text{SO}_p(3) \otimes \text{SO}_n(3) \\
 & & \searrow & & \downarrow & & \downarrow \\
 & & \text{U}(3, 3) & \longrightarrow & \text{SU}_p(3) \otimes \text{SU}_n(3) & \longrightarrow & \text{SU}^*(3) \\
 & & \searrow & & \nearrow & & \nearrow \\
 & & & & \text{U}^*(3) \otimes \text{U}(1, 1) & &
 \end{array} \quad (1)$$

Compared to the lattice given in Ref. [23], here a new reduction chain [the last one in Eq. (1)] is considered. As it can be seen, the IVBM has a very rich algebraic structure of subgroups. The first three dynamical limits of the IVBM given in Eq. (1) and the geometries corresponding to them are considered in Ref. [23]. In this paper we are concentrating on the last reduction chain of the dynamical symmetry group $\text{Sp}(12, R)$ of the IVBM for studying the triaxiality in atomic nuclei. As we will see throughout the paper, this dynamical symmetry is appropriate for nuclei in which the one type of particles is particle-like and the other is hole-like.

All bilinear operators of the creation and annihilation operators of the two kinds of vector bosons

$$u_k^\dagger(\alpha)u_m^\dagger(\beta), \quad u_k^\dagger(\alpha)u_m(\beta), \quad u_k(\alpha)u_m(\beta) \quad (2)$$

define the boson representation of the $\text{Sp}(12, R)$ algebra. We also introduce the following notations: $u_m^\dagger(\alpha = 1/2) = p_m^\dagger$ and $u_m^\dagger(\alpha = -1/2) = n_m^\dagger$. In terms of the p - and n -boson operators, the Weyl generators of the ladder representation of $\text{U}(3, 3)$ are

$$p_k^\dagger p_m, \quad p_k^\dagger n_m^\dagger, \quad -n_k p_m, \quad -n_m^\dagger n_k, \quad (3)$$

which are obviously a subset of symplectic generators (2). The first-order Casimir operator of $\text{U}(3, 3)$ is

$$C_1[\text{U}(3, 3)] = \sum_k (p_k^\dagger p_k - n_k^\dagger n_k) \quad (4)$$

and does not differ essentially from the operator T_0 defined in Ref. [23]:

$$T_0 = \frac{1}{2}C_1[\text{U}(3, 3)] + \frac{3}{2}. \quad (5)$$

The algebra $\text{U}^*(3) = \{A_{km} \equiv p_k^\dagger p_m - n_m^\dagger n_k\}$ can also be defined in the following way:

$$M = N_p - N_n, \quad (6)$$

$$L_M = L_M^p + L_M^n, \quad (7)$$

$$Q_M = Q_M^p - Q_M^n, \quad (8)$$

where the one-fluid operators entering in Eqs. (6)–(8) are given by

$$N_p = \sqrt{3}(p^\dagger \times p)^{(0)}, \quad (9)$$

$$L_M^p = \sqrt{2}(p^\dagger \times p)_M^{(1)}, \quad (10)$$

$$Q_M^p = \sqrt{2}(p^\dagger \times p)_M^{(2)}, \quad (11)$$

and

$$N_n = \sqrt{3}(n^\dagger \times n)^{(0)}, \quad (12)$$

$$L_M^n = \sqrt{2}(n^\dagger \times n)_M^{(1)}, \quad (13)$$

$$Q_M^n = \sqrt{2}(n^\dagger \times n)_M^{(2)}. \quad (14)$$

The $\text{U}(1, 1)$ generators can be obtained from the $\text{U}(3, 3)$ ones (3) simply by contraction. As shown later, the two algebras $\text{U}(1, 1)$ and $\text{U}^*(3)$ are mutually complementary within a given irreducible representation (irrep) of $\text{U}(3, 3)$ [38].

The second-order Casimir operator of $\text{U}^*(3)$ can be defined as

$$C_2[\text{U}^*(3)] = \sum_{ij} A_{ij} A_{ji}. \quad (15)$$

The $\text{SU}^*(3)$ algebra is obtained by excluding the operator (6), which is the single generator of the $\text{O}(2)$ algebra, whereas the angular momentum algebra $\text{SO}(3)$ is generated by the generators L_M only.

The $\text{U}(3, 3)$ irreps are positive-discrete-series irreps characterized by their lowest weight $\{f_3 + \frac{1}{2}, f_2 + \frac{1}{2}, f_1 + \frac{1}{2}, f'_3 + \frac{1}{2}, f'_2 + \frac{1}{2}, f'_1 + \frac{1}{2}\}$, where $\{f_1 + \frac{1}{2}, f_2 + \frac{1}{2}, f_3 + \frac{1}{2}\}$ and $\{f'_1 + \frac{1}{2}, f'_2 + \frac{1}{2}, f'_3 + \frac{1}{2}\}$ are two partitions. The lowest-weight state of such irreps is also the lowest-weight state of an irrep $\{f_1 + \frac{1}{2}, f_2 + \frac{1}{2}, f_3 + \frac{1}{2}\} \otimes \{f'_1 + \frac{1}{2}, f'_2 + \frac{1}{2}, f'_3 + \frac{1}{2}\}$ of the maximal compact subgroup $\text{U}_p(3) \otimes \text{U}_n(3)$. It turns out that there exist three cases for the partitions [38]: (i) $f_1 = \nu > 0$, $f_2 = f_3 = f'_1 = f'_2 = f'_3 = 0$; (ii) $f'_1 = -\nu > 0$, $f_1 = f_2 =$

$f_3 = f'_2 = f'_3 = 0$; and (iii) $f_1 = f_2 = f_3 = f'_1 = f'_2 = f'_3 = \nu = 0$. The $U(3, 3)$ irreps contained in either irrep $\langle(1/2)^6\rangle$ or $\langle(1/2)^5 3/2\rangle$ of $Sp(12, R)$ can be denoted by the shorthand notation $[\nu]$, $\nu \in Z$, defined as follows:

$$[\nu] = \{(1/2)^2, \nu + \frac{1}{2}; (1/2)^3\} \quad \text{if } \nu > 0, \quad (16)$$

$$= \{(1/2)^3; (1/2)^2, -\nu + \frac{1}{2}\} \quad \text{if } \nu < 0, \quad (17)$$

$$= \{(1/2)^3; (1/2)^3\} \quad \text{if } \nu = 0. \quad (18)$$

The branching rules can be written as

$$\langle(1/2)^6\rangle \downarrow \sum_{\nu=-\infty, \nu=\text{even}}^{+\infty} \oplus[\nu] \quad (19)$$

and

$$\langle(1/2)^5 3/2\rangle \downarrow \sum_{\nu=-\infty, \nu=\text{odd}}^{+\infty} \oplus[\nu]. \quad (20)$$

It can be shown [38] that the label ν specifying the $U(3, 3)$ irreps in Eqs. (16)–(20) has a very simple meaning: it is just the eigenvalue of the first-order Casimir operator (4) of $U(3, 3)$, i.e., $\nu = N_p - N_n$.

The $U^*(3)$ irreps are characterized by their highest weight $[n_1, n_2, n_3]_3$, where n_1, n_2, n_3 are some integers satisfying the inequalities $n_1 \geq n_2 \geq n_3$. We note that $[n_1, n_2, n_3]_3$ may assume negative as well as non-negative values and hence correspond to mixed irreps of $U^*(3)$ [39].

The $U(1, 1)$ irreps contained in a positive-series irrep $[\nu]$ of $U(3, 3)$ are also positive-discrete-series irreps characterized by their lowest weight $N_p + \frac{3}{2}, N_n + \frac{3}{2}$ [38]. We denote such irreps by the shorthand notation $[N_p, N_n] = \{N_p + \frac{3}{2}, N_n + \frac{3}{2}\}$. The $U(1, 1)$ and $U^*(3)$ groups are complementary within any irrep $[\nu]$ of $U(3, 3)$ or, in other words, the irreps $[N_p, N_n] \otimes [n_1, n_2, n_3]_3$ of $U(1, 1) \otimes U^*(3)$, contained in a given irrep $[\nu]$ of $U(3, 3)$, are multiplicity free and there is a one-to-one correspondence between the labels $[n_1, n_2, n_3]_3$ of the $U^*(3)$ irreps and the labels $[N_p, N_n]$ of the associated $U(1, 1)$ irreps. The precise relation is $[n_1, n_2, n_3]_3 \equiv [N_p, 0, -N_n]_3$ and $N_p - N_n = \sum_{k=1}^3 n_k = \nu$ [38]. Then the $SU^*(3)$ irreps are $(\mu, \nu) = (N_p, N_n)$. This is just the case when the one type of particles is particle-like and the other is hole-like and the corresponding algebra can be identified with the $SU^*(3)$ one defined in Refs. [24–26]. Indeed, the $SU^*(3)$ algebra can be related to the $SU(3) = \{L_M = L_M^p + L_M^n, Q_M = Q_M^p + Q_M^n\}$ one defined in Ref. [23] by means of the transformation

$$\begin{aligned} n_k^\dagger &\rightarrow n_k, \\ n_k &\rightarrow -n_k^\dagger, \end{aligned} \quad (21)$$

which actually coincides with the particle-hole conjugation. According to this the new operator n_k^\dagger of $SU^*(3)$ transforms under the conjugate $SU(3)$ representation of $(1, 0)$, namely the irrep $(0, 1)$. Thus the allowed $SU^*(3)$ representations are given by

$$(\lambda, \mu) = \sum_{k=0}^{\min(N_p, N_n)} (N_p - k, N_p - k). \quad (22)$$

This corresponds to the reduction

$$\begin{aligned} Sp(12, R) \supset U(3, 3) \\ \supset SU_p(3) \otimes SU_n(3) \supset SU^*(3) \supset SO(3), \end{aligned} \quad (23)$$

that is, through the maximal compact subalgebra $SU_p(3) \otimes SU_n(3) \supset U(3, 3)$. Consider, for example, $N_p = 2$ and $N_n = 2$; then according to Eq. (22) one finds

$$(2, 0) \otimes (0, 2) = (2, 2) + (1, 1) + (0, 0). \quad (24)$$

The $(2, 2)$ irrep contains a $K = 0$ band with $L = 0, 2$ and a $K = 2$ band with $L = 2, 3, 4$, while the $(1, 1)$ irrep contains a $K = 1$ band with $L = 1, 2$ and the $(0, 0)$ irrep contains a $K = 0$ band with only $L = 0$. It is clear that this spectrum is very different from the spectrum of $N_p = 2$ and $N_n = 2$ in the $SU(3)$ case. Whereas in the particle-particle case the ground band belongs to the $(N_p + N_p, 0)$ irrep, in the particle-hole case the ground band turns out to belong to the (N_p, N_p) irrep.

The transformation (21) corresponds to application of the transformation $Q_M^n \rightarrow -Q_M^n, L_M^n \rightarrow L_M^n$ in the n -boson $SU_n(3)$ algebra. This changes the common $SU(3)$ quadrupole operator $Q_M = Q_M^p + Q_M^n$ of the combined pn -system into that given by Eq. (8). A similar type of $SU^*(3)$ algebra for IBM-2, generated by $Q_M = Q_M^p - Q_M^n$ together with the angular momentum operators, is given in Ref. [25]. The transformation (21), being a special case of a wider class of transformations known as inner automorphisms, does not change the commutation relations of $SU(3)$ algebra; however, it changes the commutation relations of its complimentary $SU_T(2)$ algebra to those corresponding to the non-compact subalgebra $SU(1, 1) \subset Sp(12, R)$ [see Eq. (1)].

It is known that representation theory does provide all of the embeddings, but it does not provide all of the dynamical symmetries [40]. The inner automorphisms can provide new dynamical symmetry limits, sometimes referred as to “hidden” [40] or “parameter” symmetries [41]. It is shown in the next sections that the (perturbed) $SU^*(3)$ algebra provides a new physically distinct dynamical symmetry limit of the IVBM. Indeed, the geometrical interpretation of this dynamical symmetry is that of a prolate (proton) axially deformed rotor coupled to the oblate (neutron) axially deformed rotor [or vice versa, when the inner automorphism (21) is performed with respect to the p bosons], which in some circumstances corresponds to a triaxial shape of the compound nucleus in its ground-state configuration.

The most general Hamiltonian with $SU^*(3)$ symmetry consists of the Casimir invariants of $SU^*(3)$ and its subgroup $SO(3)$,

$$H = aC_2[SU^*(3)] + bC_2[SO(3)], \quad (25)$$

where

$$C_2[SU^*(3)] = \frac{1}{6}Q^2 + \frac{1}{2}L^2 \quad (26)$$

and the quadrupole operator Q is given by Eq. (8).

The spectrum of this Hamiltonian is determined by

$$H = a(\lambda^2 + \mu^2 + \lambda\mu + 3\lambda + 3\mu) + bL(L + 1). \quad (27)$$

III. SHAPE STRUCTURE

In the present paper we are interested in the shapes corresponding to the new dynamical symmetry limit. The geometry associated with a given Hamiltonian can be obtained by the coherent state method. The standard approach to obtain the geometry of the system is to express the collective variables in the intrinsic (body-fixed) frame of reference.

Within the IVBM, the (unnormalized) coherent state (CS) (or intrinsic state) for the ground-state band for even-even nuclei can be expressed as [23]

$$|N; \xi, \zeta\rangle \propto \left[\sum_k (\xi_k p_k^\dagger + \zeta_k n_k^\dagger) \right]^N |0\rangle, \quad (28)$$

where the collective variables ξ_k and ζ_k are components of three-dimensional complex vectors. For static problems these variables can be chosen real.

Usually, when some geometrical considerations concerning the choice of the intrinsic frame are taken into account, the treatment of the problem is significantly simplified. The geometry can be chosen such that $\vec{\xi}$ and $\vec{\zeta}$ to span the xz plane with the x axis along $\vec{\xi}$ and $\vec{\zeta}$ is rotated by an angle θ about the out-of-plane y axis, $\vec{\xi} \cdot \vec{\zeta} = r_1 r_2 \cos \theta$. In this way, the condensate can be parametrized in terms of two real coordinates r_1 and r_2 (the lengths of the two vectors) and their relative angle θ ($r_1, r_2 \geq 0$ and $0 \leq \theta \leq \pi$) [23]:

$$|N; r_1, r_2, \theta\rangle = \frac{1}{\sqrt{N!}} (B^\dagger)^N |0\rangle \quad (29)$$

with

$$B^\dagger = \frac{1}{\sqrt{r_1^2 + r_2^2}} [r_1 p_x^\dagger + r_2 (n_x^\dagger \cos \theta + n_z^\dagger \sin \theta)], \quad (30)$$

where $|0\rangle$ is the boson vacuum.

We simply study the $SU^*(3)$ Hamiltonian

$$H = kC_2[SU^*(3)], \quad (31)$$

expressed only by the second-order $SU^*(3)$ Casimir operator. In the present section, we set $k = -1$.

The ground-state energy surface is obtained by calculating the expectation value of the boson Hamiltonian (31) in the CS (29):

$$E(N; r_1, r_2, \theta) = \frac{\langle N; r_1, r_2, \theta | H | N; r_1, r_2, \theta \rangle}{\langle N; r_1, r_2, \theta | N; r_1, r_2, \theta \rangle}. \quad (32)$$

The equilibrium ‘‘shape’’ is determined by minimizing the energy surface with respect to r_1 , r_2 , and θ . It is convenient to introduce a new dynamical variable $\rho = r_2/r_1$ [23] as a measure of ‘‘deformation,’’ which together with the parameter θ determines the corresponding ‘‘shape.’’

The expectation value of Eq. (31) with respect to Eq. (29) gives the following energy surface:

$$E(N; \rho, \theta) = \frac{2}{3}(kN) \left[\frac{1 + \rho^4 - \rho^2(3 \cos^2 \theta - 1)}{(1 + \rho^2)^2} + 4 \right]. \quad (33)$$

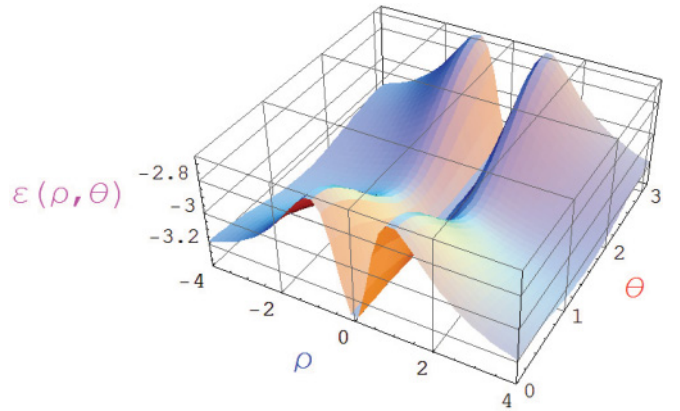


FIG. 1. (Color online) The scaled energy surface $\varepsilon(\rho, \theta)$ in the $SU^*(3)$ limit for $k = -1$.

The scaled energy $\varepsilon(\rho, \theta) = E(N; \rho, \theta)/kN$ is given in Fig. 1. From the figure, one can see that the global minimum occurs at $\rho_0 = 0$, which, as is shown further, corresponds to an oblate deformed shape.

To see to what geometry the energy surface (33) depicted in Fig. 1 corresponds, we consider the relation of the parameter θ with the commonly used asymmetry parameter γ of the geometric CM of Bohr and Mottelson. A relation between standard CM shape variables used to describe the deformation of the collective motion and the shape parameters in the intrinsic state of the IVBM can be obtained by calculating the expectation value of the quadrupole moments of the corresponding dynamical symmetry with respect to the IVBM coherent state. In the CS of the IVBM, the effective deformation γ_{eff} can be defined in the usual way as [42]

$$\tan \gamma_{\text{eff}} = \sqrt{2} \frac{\langle Q_2 \rangle}{\langle Q_0 \rangle}, \quad (34)$$

where $\langle Q_\mu \rangle$ denotes the expectation value of the μ th component of the quadrupole operator.

For the $SU^*(3)$ algebra with the generators (8) one obtains

$$\tan \gamma_{\text{eff}} = \frac{\sqrt{3}(1 - \rho^2 \cos^2 \theta)}{[-1 - \frac{\rho^2}{2}(-3 \cos 2\theta + 1)]}. \quad (35)$$

Expression (35) gives a relation between the ‘‘projective’’ IVBM CS deformation parameters $\{\rho, \theta\}$ and the standard collective model parameter γ_{eff} , determining the triaxiality of the nuclear system. From Eq. (35) it is easily seen that for the equilibrium values of the IVBM shape parameters $|\rho_0| = 0$ and θ arbitrary in the $SU^*(3)$ limit one obtains $|\gamma_{\text{eff}}| = 60^\circ$ and hence it corresponds to an oblate deformed shape.

Finally, we note that for $k > 0$ the minima of the $SU^*(3)$ energy surface (related to the maxima of Fig. 1 simply by an inversion) are at $|\rho| \neq 0$ ($|\rho| = 1$) and $\theta_0 = 0^\circ$. For $k > 0$, there is a second (local) extremum placed at $|\rho_0| = 1$ and $\theta_0 = 90^\circ$, which according to Eq. (35) corresponds to $|\gamma_{\text{eff}}| = 30^\circ$ and hence to a triaxial maximum. In the next section we see that the addition of some perturbation terms to the Hamiltonian (31) changes the structure of the energy surface and a stable triaxial minimum appears.

IV. PERTURBATION OF THE SU*(3) DYNAMICAL SYMMETRY

As it was mentioned, the exact SU*(3) symmetry shows a large degeneracy in the level spectra, which in actual nuclei is not observed. In some cases, the energy spectra can be situated between the SU*(3) and O(6) or SU(3) and SU*(3) dynamical limits. Indeed, several systematic studies [43] have shown that transitional nuclei exhibit the triaxial features. A number of signatures of γ -soft and γ -rigid structures in nuclei have been discussed [1,2,43]. In Ref. [44] it was shown that the empirical deviations from the O(6) limit of the IBM, in the Pt and Xe, Ba regions, can be interpreted by introducing explicitly triaxial degrees of freedom, suggesting a more complex and possibly intermediate situation between γ -rigid and γ -unstable properties. In this respect, we study the influence of different types of perturbations on the SU*(3) dynamical symmetry of the IVBM. We consider only the two types of perturbation terms on the SU*(3) energy surface, namely the inclusion of a Majorana interaction and an O(6) term.

A. The Majorana perturbation

The Hamiltonian, to which a Majorana term is added, takes the form

$$H_I = k \frac{1}{N-1} C_2[\text{SU}^*(3)] + a \frac{1}{N-1} M_3, \quad (36)$$

where the Majorana operator is defined as

$$M_3 = 2(p^\dagger \times n^\dagger)^{(1)} \cdot (p \times n)^{(1)} \quad (37)$$

and it is related to the U(3) second-order Casimir invariant $C_2[\text{U}(3)]$ via the relation

$$C_2[\text{U}(3)] = N(N+2) - 2M_3. \quad (38)$$

In Eq. (36) the appropriate scaling factors in N are included.

The classical limit of the Majorana term (37) is given by the following expression:

$$E(N; \rho, \theta) = aN(N-1) \frac{\rho^2 \sin^2 \theta}{(1+\rho^2)^2}. \quad (39)$$

The scaled energy surface of the Hamiltonian (36) [Eqs. (33) and (39)] is shown in Figs. 2 and 3 in the form of a three-dimensional plot and a contour plot, respectively. The values of the model parameters used are $k = -1$, $a = -3$. From the figures, according to Eq. (35), it is clear that a stable triaxial minimum results at $\theta_0 = 90^\circ$ and $|\rho_0| = 1$, which becomes deeper and deeper with the increasing absolute value of the parameter a .

The inspection of the energy surfaces for different values of the parameter a (at fixed $k = -1$) shows that, for small negative values of the parameter a ($|a| \leq 0.4$) and realistic values of $\rho \in [0, 1.5]$, the minimum is at $\rho_0 = 0$, corresponding to an oblate deformed shape. In the interval $|a| \approx 0.5-0.8$ there exist two degenerate minima at $|\rho_0| = 0$ and $|\rho_0| = 1$, $\theta_0 = 90^\circ$, respectively, while for $a \leq -0.86$ a stable triaxial minimum ($\theta_0 = 90^\circ$, $|\rho_0| = 1$) occurs. This triaxial minimum persists and for positive values of the parameter k ($k = 1$)

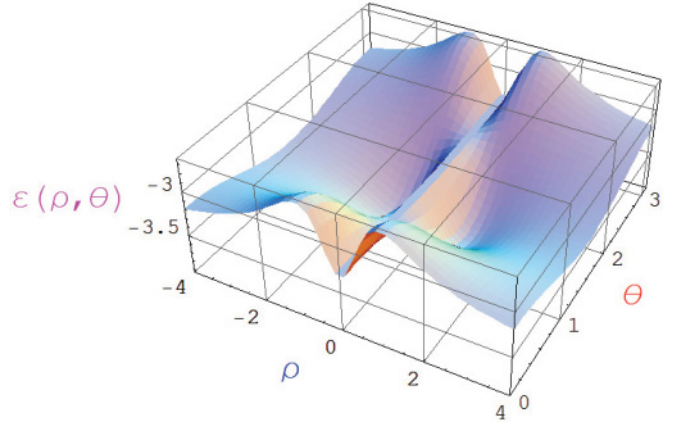


FIG. 2. (Color online) The scaled energy surface $\varepsilon(\rho, \theta)$ in the SU*(3) limit, when a Majorana term is added. The values of the model parameters used are $k = -1$, $a = -3$.

when $a < -2$, and also becomes more pronounced with the further increasing of the absolute value of a .

In the present work we are mainly interested in the ground-state properties of the energy surfaces considered. Nevertheless, to see to what extent the structure of the theoretical energy levels corresponds to a real experimental pattern and how the energy spectrum generated by the pure SU*(3) Hamiltonian (31) is influenced by the inclusion of the Majorana interaction, we consider the following Hamiltonian:

$$H = kC_2[\text{SU}^*(3)] + k'C_2[\text{SO}(3)] + aM_3, \quad (40)$$

where the rotational term in Eq. (40) is added to lift the degeneracy of the states with different angular momentum.

In Fig. 4 we plot the theoretical predictions for the ground-state band, γ band, and $K^+ = 4^+$ band energies, obtained with the Hamiltonian (40) with the following values of the model parameters: $k = -0.0136$ MeV, $k' = 0.0343$ MeV and $a = -0.0131$ MeV. The values of the latter are determined by

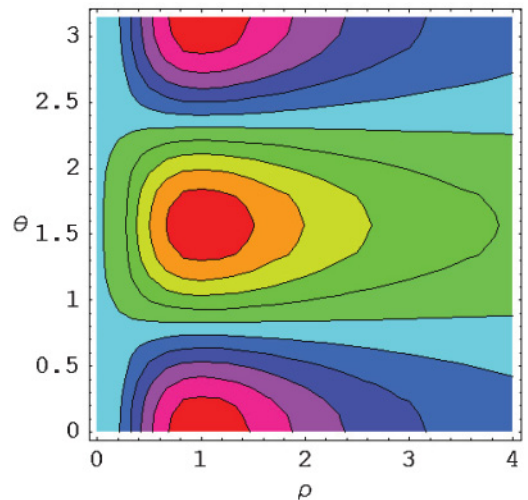


FIG. 3. (Color online) Contour plot of the scaled energy surface $\varepsilon(\rho, \theta)$ in the SU*(3) limit, when a Majorana term is added. The values of the model parameters used are $k = -1$, $a = -3$. Only the region $\rho > 0$ is depicted.

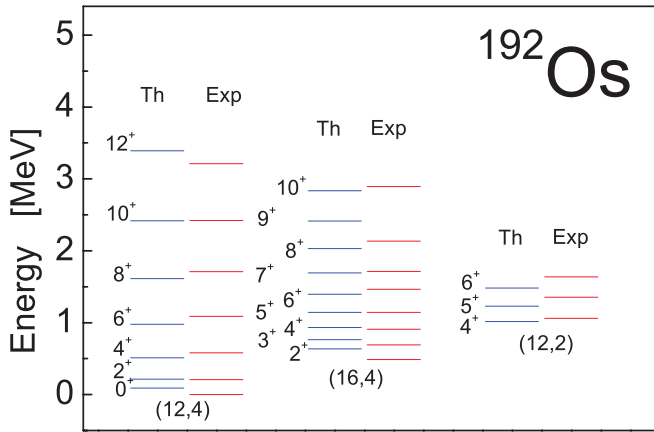


FIG. 4. (Color online) Detailed energy spectrum, obtained with the Hamiltonian (40), corresponding to the parameters $k = -0.0136$ MeV, $k' = 0.0343$ MeV, and $a = -0.0131$ MeV, compared with the experimental data for ^{192}Os . Different $\text{SU}^*(3)$ irreps associated with the bands under consideration are also indicated. Data are taken from Refs. [6,45].

using a minimization χ^2 procedure. The theoretical results are compared to the experimental data [6,45] for the ^{192}Os nucleus. The latter is considered in the literature (see, e.g., Refs. [2,6]) as being a triaxial one. From the figure one can see that the theoretical predictions are far from perfect [especially for the

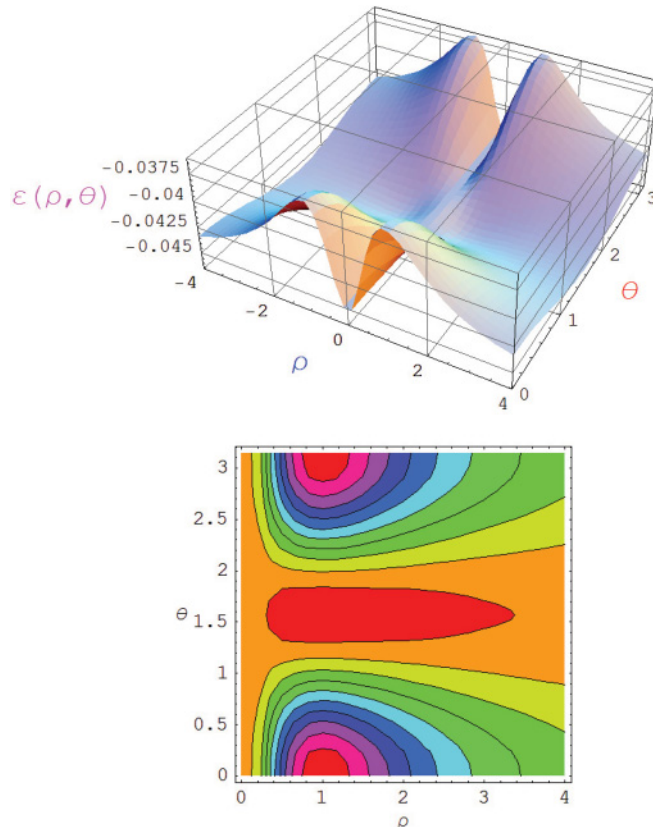


FIG. 5. (Color online) The scaled ground-state energy surface $\varepsilon(\rho, \theta)$ in ^{192}Os for the model parameters obtained in the fitting procedure in the form of (top) three-dimensional and (bottom) contour plots.

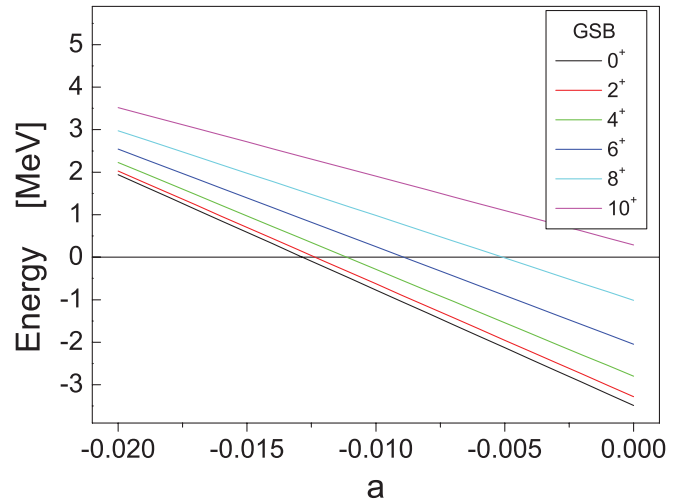


FIG. 6. (Color online) The ground-state band (GSB) for the Hamiltonian (40) as a function of the strength parameter a . The values of the rest of the model parameters are $k = -0.0136$ MeV, $k' = 0.0343$ MeV. The $\text{SU}^*(3)$ irrep corresponding to the GSB is (12, 4).

ground-state band (GSB)], but nevertheless the structure of the energy spectrum of ^{192}Os is reasonably reproduced in general. The fit is performed for all states of the ground-state band and γ band simultaneously. That is why we obtain average fits along the entire bands, and the states at the bottom for these two bands are overestimated.

The quality of the obtained results is not surprising taking into account the very simple form of the Hamiltonian that is used. The improvement of the theoretical results obviously requires a more realistic interaction, which should be incorporated into the model Hamiltonian. As we said, the present work is focused on the ground-state properties of the energy surface and the calculations carry a very schematic character.

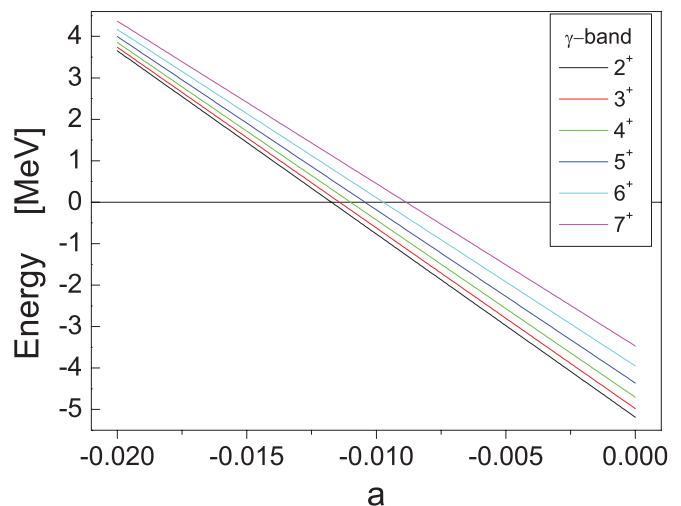


FIG. 7. (Color online) The γ band for the Hamiltonian (40) as a function of the strength parameter a . The values of the rest of the model parameters are $k = -0.0136$ MeV, $k' = 0.0343$ MeV. The $\text{SU}^*(3)$ irrep corresponding to the γ band is (10, 6).

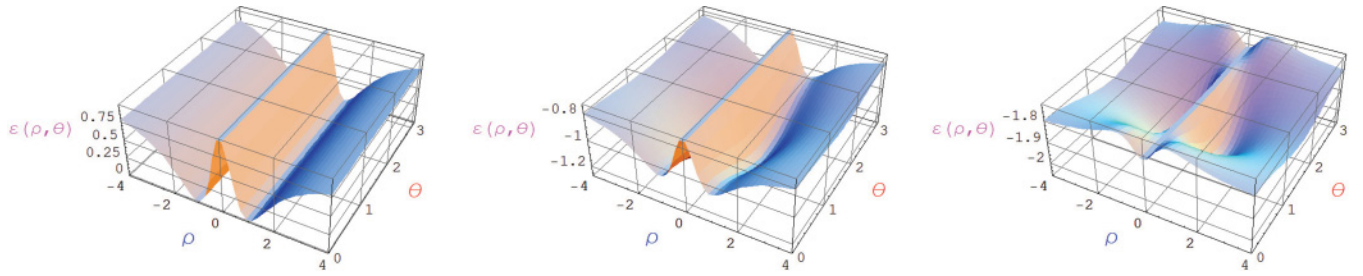


FIG. 8. (Color online) The scaled energy surface $\varepsilon(\rho, \theta)$ corresponding to the Hamiltonian (41) for $g = 0, 0.4$, and 0.65 , respectively.

We plot the ground-state energy surface in ^{192}Os for the model parameters obtained in the fitting procedure in the form of three-dimensional and contour plots in Fig. 5. From the figure one can see that a very shallow triaxial minimum for the ground state in ^{192}Os is observed, which corresponds to $\gamma_{\text{eff}} = 30^\circ$. The latter is separated from the neighboring oblate minimum by only $\simeq 1$ keV (see the energy scale in Fig. 5); that is, the two observed minima are practically degenerate. From the contour plot in Fig. 5 it can be seen that this extremely shallow triaxial minimum is soft along the θ direction, which corresponds to γ softness (the change of ρ at fixed $\theta_0 = 90^\circ$ changes the asymmetry parameter γ_{eff}). The structure of the energy surface obtained in our schematic calculations for ^{192}Os supports the consideration of this nucleus as being a transitional one between axially symmetric prolate and oblate deformed ones, passing through a γ -soft triaxial region. Indeed, some theoretical calculations [17,46] predict a very tiny region of triaxiality between the prolate and oblate shapes. The self-consistent Hartree-Fock-Bogoliubov calculations with Gogny D1S and Skyrme SLy4 forces predict that the prolate-to-oblate transition takes place at neutron number $N = 116$, i.e., exactly the case for ^{192}Os .

The evolution of the ground-state band and γ band for the Hamiltonian (40) as a function of the strength parameter a is shown in Figs. 6 and 7, respectively. The values of the rest of the model parameters are kept the same as given above. From the figures one can see that the inclusion of the Majorana term does not change the level spacings for either the ground state

or the γ bands and hence preserves the character of the bands. One can see also that the energy levels of both the GSB and the γ band are affected in the same manner as a function of the strength of the Majorana interaction.

B. Phase transition between O(6) and $SU^*(3)$ limits

The transition from the $SU^*(3)$ to the O(6) limit can be realized by the following Hamiltonian:

$$H_{\text{II}} = (1 - g) \frac{1}{N - 1} P^\dagger P - g \frac{1}{N - 1} C_2[SU^*(3)], \quad (41)$$

varying the parameter g from $g = 0$ (O(6) γ -unstable limit) to $g = 1$ ($SU^*(3)$ limit). The O(6) pairing operator is defined as $P^\dagger = \frac{1}{2}(p^\dagger \cdot p^\dagger - n^\dagger \cdot n^\dagger)$. The $P^\dagger P$ operator in Eq. (41) is related to the quadratic Casimir operator $C_2[\text{O}(6)]$ of O(6) by the equation $C_2[\text{O}(6)] = -4P^\dagger P + N(N + 4)$.

In Fig. 8 we show the scaled energy surfaces corresponding to the Hamiltonian (41) for three different values of g , namely $g = 0, 0.4$, and 0.65 , respectively. For $g = 0$ we have the typical energy surface for the γ -unstable deformed shape.

The evolution of the energy surfaces for the same values of the parameter g is shown as contour plots in Fig. 9. Numerical studies show that the triaxial minimum ($\theta_0 = 90^\circ, |\rho_0| = 1$) persists for the values of g in the interval $0 < g \leq 0.85$, where for small values of g it is very shallow and becomes more pronounced with the increase of g (up to $g \approx 0.8$). From Fig. 8 it can be seen that a second local minimum appears at $\rho_0 = 0$ for $g = 0.65$. Around $g \sim 0.84$ the two

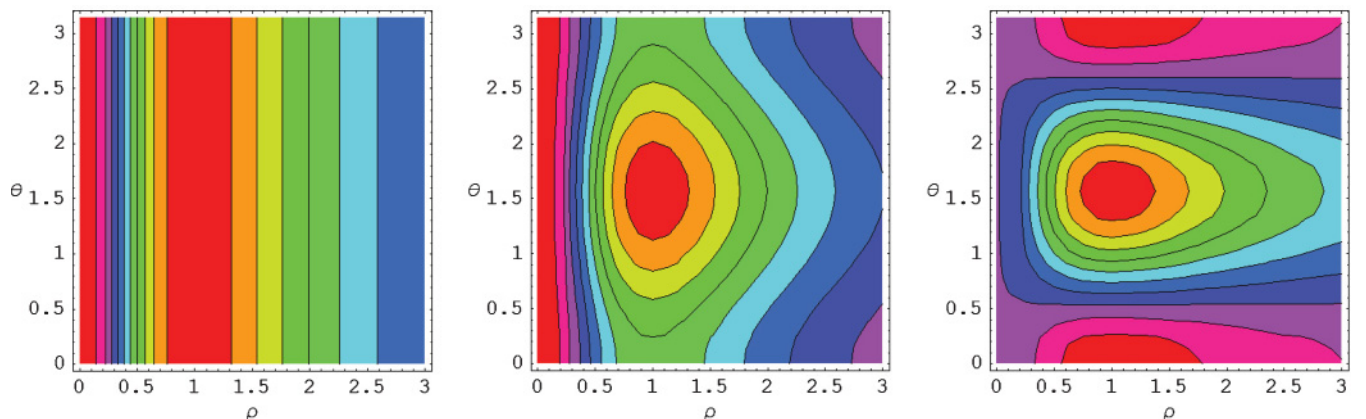


FIG. 9. (Color online) A contour plot of the scaled energy surface $\varepsilon(\rho, \theta)$ corresponding to the Hamiltonian (41) for $g = 0, 0.4$, and 0.65 , respectively. Only the region $\rho > 0$ is depicted.

minima become degenerate (up to $g \simeq 0.88$) and for $g \geq 0.89$ the second minimum at $\rho_0 = 0$ becomes a global one in the interval $\rho \in [0, 1.5]$ [just as in the case when the $SU^*(3)$ symmetry is perturbed by the Majorana interaction for comparatively small values of the parameter a , $|a| < 0.7$]. The geometry of the $SU^*(3)$ ($g = 1$) limit for $\rho_0 = 0$, as was mentioned, corresponds to that of an oblate deformed rotor ($|\gamma_{\text{eff}}| = 60^\circ$).

From the results obtained in the last two sections it can be concluded that the two types of perturbations disturb the exact $SU^*(3)$ symmetry energy surface in a similar way and lead to the same geometrical structure underlying both Hamiltonians under consideration.

V. SUMMARY

A new dynamical symmetry limit of the two-fluid interacting vector boson model, defined through the chain $Sp(12, R) \supset U(3, 3) \supset U^*(3) \otimes SU(1, 1) \supset SU^*(3) \supset SO(3)$, is introduced. The $SU^*(3)$ algebra considered in the present paper closely resembles many properties of the $SU^*(3)$ limit of IBM-2, which have been shown by many authors geometrically to correspond to the rigid triaxial model.

We studied the influence of different types of perturbations on the $SU^*(3)$ dynamical symmetry energy surface. In

particular, the addition of a Majorana interaction and an $O(6)$ term to the model $SU^*(3)$ Hamiltonian is investigated. It is shown that the effect of these perturbations results in the formation of a stable triaxial minimum in the energy surface of the IVBM Hamiltonian under consideration.

The effect of the Majorana interaction on the energy levels of the ground-state band and the γ band is studied as well. Using a schematic Hamiltonian (possessing a disturbed $SU^*(3)$ dynamical symmetry), the theory is applied for the calculation of the low-lying energy spectrum of the nucleus ^{192}Os , which is considered in the literature as being triaxial. The theoretical results obtained agree reasonably with the experimental data and show a very shallow triaxial minimum in the energy surface for the ground state in ^{192}Os . This suggests that the proposed dynamical symmetry might be appropriate for the description of the collective properties of different nuclei, exhibiting triaxial features. More investigations in this direction are further required.

ACKNOWLEDGMENT

This work was supported by the Bulgarian National Foundation for scientific research under Grant No. DID-02/16/17.12.2009.

-
- [1] N. V. Zamfir and R. F. Casten, *Phys. Lett. B* **260**, 265 (1991).
 [2] E. A. McCutchan, D. Bonatsos, N. V. Zamfir, and R. F. Casten, *Phys. Rev. C* **76**, 024306 (2007).
 [3] L. Wilets and M. Jean, *Phys. Rev.* **102**, 788 (1956).
 [4] A. S. Davydov and G. F. Filippov, *Nucl. Phys.* **8**, 237 (1958).
 [5] I. Yigitoglu and D. Bonatsos, *Phys. Rev. C* **83**, 014303 (2011).
 [6] A. A. Raduta and P. Baganu, *Phys. Rev. C* **83**, 034313 (2011).
 [7] D. J. Rowe, T. A. Welsh, and M. A. Caprio, *Phys. Rev. C* **79**, 054304 (2009).
 [8] M. A. Caprio, *Phys. Lett. B* **672**, 396 (2009).
 [9] K. Heyde, P. Van Isacker, M. Waroquier, and J. Moreau, *Phys. Rev. C* **29**, 1420 (1984).
 [10] G. Thiamova, *Eur. Phys. J. A* **45**, 81 (2010).
 [11] S. Kuyucak and I. Morrison, *Phys. Lett. B* **255**, 305 (1991).
 [12] P. Van Isacker, A. Bouldjedri, and S. Zerguine, *Nucl. Phys. A* **836**, 225 (2010).
 [13] A. E. L. Dieperink, *Nucl. Phys. A* **421**, 189c (1984).
 [14] M. A. Caprio and F. Iachello, *Phys. Rev. Lett.* **93**, 242502 (2004).
 [15] J. M. Arias, J. E. Garcia-Ramos, and J. Dukelsky, *Phys. Rev. Lett.* **93**, 212501 (2004).
 [16] P. Cejnar and J. Jolie, *Prog. Part. Nucl. Phys.* **62**, 210 (2009).
 [17] L. Fortunato, C. E. Alonso, J. M. Arias, J. E. Garcia-Ramos, and A. Vitturi, *Phys. Rev. C* **84**, 014326 (2011).
 [18] A. Arima, T. Otsuka, F. Iachello, and I. Talmi, *Phys. Lett. B* **66**, 205 (1977).
 [19] F. Iachello, *Phys. Rev. Lett.* **91**, 132502 (2003).
 [20] A. I. Georgieva, H. G. Ganev, J. P. Draayer, and V. P. Garistov, *Phys. Part. Nucl.* **40**, 469 (2009).
 [21] D. J. Rowe, *Rep. Prog. Phys.* **48**, 1419 (1985).
 [22] G. Rosensteel and D. J. Rowe, *Phys. Rev. Lett.* **38**, 10 (1977); *Int. J. Theor. Phys.* **16**, 63 (1977); *Ann. Phys. (NY)* **126**, 343 (1980).
 [23] H. G. Ganev, *Phys. Rev. C* **83**, 034307 (2011).
 [24] A. E. L. Dieperink and R. Bijker, *Phys. Lett. B* **116**, 77 (1982).
 [25] N. R. Walet and P. J. Brussaard, *Nucl. Phys. A* **474**, 61 (1987).
 [26] A. Sevrin, K. Heyde, and J. Jolie, *Phys. Rev. C* **36**, 2621 (1987).
 [27] R. F. Casten and D. D. Warner, *Rev. Mod. Phys.* **60**, 389 (1988).
 [28] V. Bargmann and M. Moshinsky, *Nucl. Phys.* **18**, 697 (1960); **23**, 177 (1961).
 [29] A. I. Georgieva, P. Raychev, and R. Rouseev, *J. Phys. G* **8**, 1377 (1982).
 [30] R. M. Asherova *et al.*, *J. Phys. G: Nucl. Part. Phys.* **19**, 1887 (1993).
 [31] F. Iachello and I. Talmi, *Rev. Mod. Phys.* **59**, 339 (1987).
 [32] C. L. Wu, Da Hsuan Feng, X. G. Chen, J. Q. Chen, and M. W. Guidry, *Phys. Rev. C* **36**, 1157 (1987); P. Hals and Z. Y. Pan, *ibid.* **36**, 1212 (1987).
 [33] T. Otsuka, *Phys. Lett. B* **182**, 256 (1986).
 [34] J. Engel and F. Iachello, *Nucl. Phys. A* **472**, 61 (1987).
 [35] F. Catara, M. Sambataro, A. Insolia, and A. Vitturi, *Phys. Lett. B* **180**, 1 (1986).
 [36] F. Iachello and A. D. Jackson, *Phys. Lett. B* **108**, 151 (1982); H. Daley and F. Iachello, *ibid.* **131**, 281 (1983); H. Daley and B. Barrett, *Nucl. Phys. A* **449**, 256 (1986).
 [37] A. I. Georgieva, H. G. Ganev, J. P. Draayer, and V. P. Garistov, *J. Phys. Conf. Ser.* **128**, 012032 (2008).
 [38] C. Quesne, *J. Phys. A: Math. Gen.* **19**, 2689 (1986).

- [39] J. Flores, *J. Math. Phys.* **8**, 454 (1967); J. Flores and M. Moshinsky, *Nucl. Phys. A* **93**, 81 (1967).
- [40] D. Kusnezov, *Phys. Rev. Lett.* **79**, 537 (1997).
- [41] A. M. Shirokov, N. A. Smirnova, and Yu. F. Smirnov, *Phys. Lett. B* **434**, 237 (1998).
- [42] A. Bohr and B. R. Mottelson, *Nuclear Structure* (W. A. Benjamin, New York, 1975), Vol. II.
- [43] Liao Ji-zhi, *Phys. Rev. C* **51**, 141 (1995); C. Bihari *et al.*, *Phys. Scr.* **77**, 055201 (2008); **78**, 045201 (2008); M. Varshney, *ibid.* **83**, 015201 (2011).
- [44] R. F. Casten *et al.*, *Nucl. Phys. A* **439**, 289 (1985).
- [45] C. Y. Wu *et al.*, *Nucl. Phys. A* **607**, 178 (1996).
- [46] L. M. Robledo, R. Rodriguez-Guzman, and P. Sarriguren, *J. Phys. G: Nucl. Part. Phys.* **36**, 115104 (2009).